Journal of Power Sources 500 (2021) 229949

Contents lists available at ScienceDirect

Journal of Power Sources

journal homepage: www.elsevier.com/locate/jpowsour

Microstructure and electrochemical behavior of layered cathodes for molten carbonate fuel cell

K. Ćwieka [a,*], A. Lysik [a], T. Wejrzanowski [a], T. Norby [b], W. Xing [c]

[a] Warsaw University of Technology, Faculty of Materials Science and Engineering, Woloska 141, 02-507 Warsaw, Poland
[b] Department of Chemistry, Centre for Materials Science and Nanotechnology, University of Oslo, NO-0318 Oslo, Norway
[c] SINTEF Materials and Chemistry, Sector for Sustainable Energy Technology, Forskningsveien 1, NO-0314 Oslo, Norway

HIGHLIGHTS

- New layered MCFC cathodes were designed, manufactured and characterized.
- Presence of porous silver layer decreases charge transfer resistance of MCFC cathode.
- Presence of nickel foam decreases mass transfer resistance of MCFC cathode.
- The combined effects of silver layer and nickel foam is demonstrated.

ARTICLE INFO

Keywords:
Cathode
Molten carbonate fuel cell
Microstructure
Nickel foam
Electrochemical impedance spectroscopy

ABSTRACT

In the present paper, we demonstrate how modifications of the microstructure and the chemical composition can influence the electrochemical behavior of cathodes for molten carbonate fuel cells (MCFCs). Based on our experience, we designed new MCFC cathode microstructures combining layers made of porous silver, nickel oxide or nickel foam to overcome common issues with the internal resistance of the cell. The microstructures of the standard NiO cathode and manufactured cathodes were extensively investigated using scanning electron microscopy (SEM) and porosity measurements. The electrochemical behavior and overall cell performance were examined by means of electrochemical impedance spectroscopy and single-cell tests in operation conditions. The results show that a porous silver layer tape cast onto standard NiO cathode and nickel foam used as a support layer for tape cast NiO porous layer substantially decrease resistance components representing charge transfer and mass transport phenomena, respectively. Therefore, it is beneficial to combine them into a three-layer cathode since it facilitates separation of predominant physio-chemical processes of gas and ions transport in respective layers ensuring high efficiency. The superiority of the three-layer cathode has been proven by low impedance and high power density as compared to standard NiO cathode.

1. Introduction

Molten carbonate fuel cells (MCFCs), beside solid oxide fuel cells (SOFCs), belong to the group of most promising high temperature and high performance energy converters [1–7]. Fuel cells convert chemical energy of the fuel (hydrogen, hydrogen-rich mixtures or hydrocarbons including biofuels [8–10]) into electricity (and heat) with high efficiency (even 60–80% in combination with e.g. steam turbines) thereby making them prospective to serve as unconventional, distributed clean energy sources [11,12]. As the researchers continuously investigate physio-chemical processes governing the fuel cell performance in detail, new modifications of cell components are proposed, particularly in terms of the microstructure and the chemical composition of applied materials.

A major part of published reports on the enhancement off MCFC overall performance is focused on the cathode which is deemed the most demanding cell compartment. The cathode catalyzes oxygen reduction and reaction of its activated species with carbon dioxide toward formation of carbonate ions (CO_3^{2-}) which are further transported through the electrolyte melt toward the anode, where they oxidize the fuel (hydrogen) and produce free electrons [13]. The cathode reaction is commonly considered more complex and slower than anode reaction due to oxygen reduction regarded as a rate determining step [14,15]. The most common material which the MCFC cathode is made of is nickel, in situ oxidized and lithiated to $Li_xNi_{1-x}O$ which provides sufficient catalytic activity at MCFC operating temperature (650 °C) as

* Corresponding author.
E-mail address: karol.cwieka@pw.edu.pl (K. Ćwieka).

https://doi.org/10.1016/j.jpowsour.2021.229949
Received 25 January 2021; Received in revised form 22 March 2021; Accepted 20 April 2021
Available online 7 May 2021

well as electrical conductivity and chemical stability [13], and it is a cheaper alternative to noble metals like gold or platinum.

The cathode microstructure of open porous sinter should be properly designed and carefully controlled to facilitate physio-chemical processes involved as well as achieving high performance of the cell. The pore structure must be controlled since the MCFC operation strongly depends on efficient gas transport and balance in capillary pressures within the pores of electrodes and the electrolyte matrix [16–18]. Thus, the porous cathode should be permeable for the reacting gases and not hinder their flow or access to the active sites on the catalyst surface. According to the theoretical concept, an interface between gas, electrode, and electrolyte, i.e. triple phase boundary (TPB) [19], is the active site for electrochemical reactions in the fuel cell, and the total length of the TPB within the electrode as well as access of gases to the TPB should be optimized in order to improve electrode performance [20–22].

The parameters being of the greatest importance for the efficient mass transport are porosity, mean pore size, and pore size distribution. Based on our previous experimental results, we demonstrated the higher porosity of the cathode, the better overall fuel cell performance can be induced [23]. Intentional introduction of pore size variation to the MCFC cathode, in turn, diversifies the transport pathways. Larger pores enable efficient gas transport and, therefore, facilitate permeability [24–26]. The smaller pores, flooded by the electrolyte via capillary actions, constitute pathways for the ion conduction through the carbonate melt. The fraction of smaller pores should have a size near critical for capillary action maintaining proper electrolyte uptake and immobilization [27,28]. Bi-modal pore structure of the MCFC cathode also contributes to enhancement of the performance as it determines other geometric factors that shapes catalytic active surface and mass-transport pathways i.e. specific surface area (S_V) [17], tortuosity and constrictivity of the pore channels [29,30]. Increment of the S_V also increases the TPB length and the density of active sites for electrode reactions which strongly promotes fuel cell operational efficiency and performance [31]. In the article [32] we demonstrated that, beside the triple phase boundary density (TPBD), electrolyte specific surface area (ESSA) is the important factor determined by the electrode microstructure and affecting the overall MCFC performance. We have also demonstrated a novel approach to structure ordering for high temperature fuel cell electrodes by investigating cathode including two layers characterized by different porosity, mean pore size and pore size variation. This microstructure is intended to sufficiently facilitate the phenomena governing fuel cell performance due to separation of them between particular layers (conventional cathode layer for the electrolyte uptake, nickel foam as gas-diffusion layer and mechanical support) [33].

Beside the porous microstructure, also the tuning of the chemical composition of the MCFC cathode were scrutinized toward the maximization of the performance [13,34]. As mentioned before, no real alternative has been found to date for nickel powder (in situ oxidized and lithiated — $Li_xNi_{1-x}O$) as a base material for MCFC cathode fabrication [13]. The chemical composition of the MCFC cathode is still the subject of interest for possible modifications through additives [35,36] or coatings [37–40] in order to increase both its performance and longevity (chemical stability). One of the most attractive elements found to reduce resistance and enhance performance of the cathode due to its high electrical conductivity and catalytic activity toward reactions with oxygen is silver [41,42]. Moreover, it remains thermodynamically stable in an oxygen-rich gas conditions and in the temperature range of MCFC operation i.e. 650–700 °C. In the initial stage of MCFC development, silver cathodes were used as reference electrodes during experimental testing [43,44]. Further studies of the Ag addition, improvement of the cathode polarization and enhancement of cell performance, via impedance spectroscopy, mostly attributed these positive effects to the reduction of the electron charge transfer resistance, and a significant improvement of the oxygen reduction activity (even for SOFCs [45–47]). Besides that, an Ag coated NiO cathode reported in [48] may operate efficiently at the reduced temperature (between 600 and 620 °C) as well as the partial pressure of oxygen without affecting the performance. By comparison, in our previous study, the cathode has been fabricated by tape casting of porous Ag layer onto conventional NiO layer. However, the effect was similar and was manifested in substantially lowered resistance components and higher maximum power density of NiO+Ag cathode compared to the NiO counterpart [49]. The positive effect was intensified in our work since Ag onto NiO surface is not exposed to the electrolyte (cf. [48]), but is a separate layer not infiltrated by the electrolyte.

Electrochemical impedance spectroscopy (EIS) is a powerful tool for characterization of energy conversion or storage devices like fuel cells or batteries [50,51]. It is broadly utilized to measure impedance of the cells, which can be further fitted to an equivalent circuit – a physical model of electric circuit of adequate impedance characteristics. Based on the fitting, resistances can be calculated as well as capacitances, inductances depending on the selection of circuit components which must be adequate physical representations of physio-chemical processes occurring in operando. The most common processes and phenomena to be identified are e.g. formation of double layer(s), charge transfer, ohmic losses, ion diffusion, surface exchange and bulk diffusion [52,53]. Quantitative analysis of the fittings to analogous equivalent circuits enables comparison of analyzed materials and investigation of the influence of varying material characteristics on their electrochemical behavior. In the paper [54], Authors reported the systematic study of the current–voltage and extensive EIS measurements (using modified Randles equivalent circuit) for MCFC used for carbon dioxide separator application. The measurements were performed in various gas conditions (various concentrations of H_2O, CO_2 and O_2 in the cathode feeding gas mixture) corresponding to exhaust gaseous stream. The influence of variances in concentration of each gas was investigated, as well as the aspect of aging of the cell — degradation of output parameters after long-term operation.

In the present paper, we demonstrate how simultaneous modifications of the microstructure and the chemical composition of MCFC cathode can determine its electrochemical behavior. As a reference, the conventional, one-layer nickel oxide cathode has been used. Then, two bi-layer variants were investigated as combinations of this nickel oxide layer with porous silver layer tape cast onto it, and with metallic (nickel) foam as supporting layer. Finally, in the last studied variant, we combined them into novel, three-layer cathode including porous silver, metallic foam and porous nickel oxide layers. The microstructures of the cathodes were examined after firing using scanning electron microscopy (SEM) and porosity measurements. Voltage–current characteristics were measured during the MCFC single-cell operation and the resistance behavior was examined by means of electrochemical impedance spectroscopy (EIS). The analysis of EIS results enabled us to attribute the changes in resistance components to the analyzed microstructure or chemical composition modifications of the cathodes. Therefore, porous silver layer tape cast onto conventional nickel oxide cathode as well as nickel foam used as a support layer for tape cast nickel oxide porous layer particularly reduce charge-transfer and mass-transport resistances, respectively. After combining these layers into cathode with three-layer structure, the lowest impedance characteristics and the highest power density were obtained during the measurements. The designed structure is proven beneficial in terms of separation of the predominant physio-chemical processes (gas and ions transport), which determine MCFC performance, in respective layers. This allows ensuring their high efficiency and avoiding their self-limitation.

2. Materials and methods

2.1. Materials preparation

All components of MCFC assembly (cathodes, anodes and matrices) were fabricated via tape casting of green tapes from a slurry [17,18].

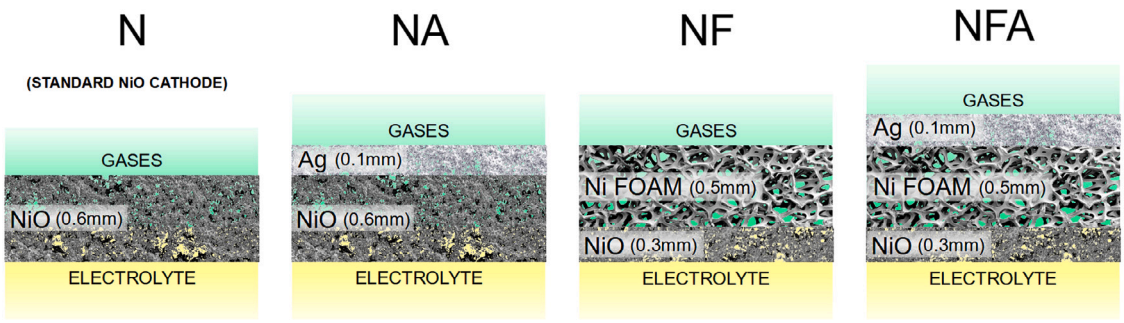

Fig. 1. Scheme of microstructure design of analyzed cathodes, their installation in the cell assembly and thicknesses of the layers. (For interpretation of the references to colour in this figure legend, the reader is referred to the web version of this article.)

Table 1
Composition of the cathode layers.

Constituent	Layer					
	NiO		Nickel foam		Silver	
	Substance	wt. %	Substance	wt. %	Substance	wt. %
Solvent	Distilled water	44.0			Distilled water	28.0
Binders	CMC	1.0			CMC	1.0
	Methocel	1.0			Methocel	1.0
Plasticizers	PEG400	3.5	n.a.	n.a.	PEG400	3.5
	Glycerol	4.5			Glycerol	5.0
Porogens	Starch	5.5			Starch	10.0
	PVB	1.5			PVB	0.0
Defoamer	Agitan DF6420	0.5			Agitan DF6420	0.5
Base material	Nickel powder	38.5	Nickel foam	100	Silver powder	50.5

Cathode and anode green tapes were also subjected to subsequent firing and sintering processes. Electrolyte was applied as a mixture of carbonate powders.

Beside the standard porous NiO cathode (hereinafter indicated as N) [17], three new variants of MCFC cathode with layered microstructure were designed and manufactured. The cathodes are hereinafter indicated as: NA (NiO layer + Ag layer) [49], NA (NiO layer + Ni foam layer) [33], and NFA (NiO layer + Ni foam layer + Ag layer). The particular layers are intended to facilitate adequate physio-chemical processes during MCFC operation, thus they must be appropriately mounted in the cell assembly with regard to the gasses and the electrolyte — see Fig. 1. In the newly designed, layered cathodes (NA, NF, NFA), the NiO layer always faces the electrolyte.

In the designed cathodes NiO and Ag layers were tape cast, and the Ni foam layer was commercially available product (Gelon Lib Co. Ltd., 0.5 mm thick, 100 ppi, surface density 250 g cm^{-2}). The slurries for NiO and silver layers were composed of solvent (distilled water), binders (carboxymethyl cellulose — CMC, Alfa Aesar, and hydroxymethyl cellulose — Methocel, CIECH), plasticizer (polyethylene glycol — PEG400 and glycerol), defoamer (AGITAN DF6420). The porogens, polyvinyl butyral (PVB — Mowital B60H, Kuraray) and starch, were added to shape the porosity and pore size variation of cathodes. Base powders for NiO and Ag layer were nickel powder (purity 99.9%, APS 5–7 μm; T255^{TM}, Vale) and Ag powder (purity 99.9%, APS 4–7 μm; Alfa Aesar) respectively — details in Table 1.

The slurries were homogenized using Planetary Centrifugal Vacuum Mixer THINKY ARV-930TWIN. The as-prepared slurries were formed onto a flat surface or directly onto another layer (tape cast NiO or Ni foam) and dried at ambient temperature for 24 h to obtain green tapes.

Finally, the green tapes were subjected to a three-stage heat treatment (1) annealing at 200 °C for 2 hours in order to remove volatile compounds, then (2) heating at 400 °C for another 2 hours to burn out the organic compounds (polymeric binders), and (3) sintering at 800 °C for 1 hour to form final porous backbones due to powder sintering. Steps 1 and 2 of the heat treatment process were carried out in an atmosphere of air, and step 3 — in a reducing atmosphere of a N_2/5% H_2 mixture.

2.2. Materials characterization

At the first stage of the materials preparation, particle size distributions (PSD) of nickel and silver powders were measured using laser diffraction analysis (HORIBA LA-950).

Scanning electron microscope (SEM; SU8000) observations in secondary electrons (SE) mode revealed the morphology of powders, microstructures of Ni foam and cathodes in pristine condition (after firing). Backscattered electrons (BSE) mode, in turn, was applied to observe the differences in the chemical composition of particular layers using phase contrast. Porosity was measured based on the Archimedes' principle (according to ASTM B962 13).

2.3. Single-cell tests and electrochemical impedance spectroscopy

To evaluate the influence of the microstructure on the electrochemical behavior of the cathodes, experimental investigations using single-cell tests and electrochemical impedance spectroscopy measurements have been conducted. Both measurements have been performed for each cathode in the ProboStat (Norwegian Electro Ceramics AS; norecs.com) sample holder (scheme depicted in Fig. 2a).

The assemblies for single-cell performance tests with an effective electrode area of 1 cm^2 were arranged by stacking the green sheets of matrix (γ-$LiAlO_2$) and electrolyte (lithium and potassium carbonate (Li_2CO_3)62/(K_2CO_3)38% mixture) between the sintered nickel anode and cathode (N, NA, NF or NFA) covered with current collectors (gold wire mesh) — see Fig. 2b. The scheme of the cathodes and detailed configuration of cell assembly for single-cell tests are depicted in Figs. 1 and 2b, respectively. The component assembly was then placed between gold covered plates (316 stainless steel) equipped with gas channels. In a first stage, "cell conditioning" was conducted to provide removal of organic binders by thermal decomposition. The cell was heated to 550 °C at the rate of 3 °C min^{-1} in an atmosphere of 10% CO_2/20% O_2 balanced by N_2 (flow rate of 50 ml min^{-1}) at the cathode side and anode side. At about 500 °C the ceramic matrix and electrodes were soaked with carbonate electrolyte to the desired extent. After the conditioning process the measurements were performed at

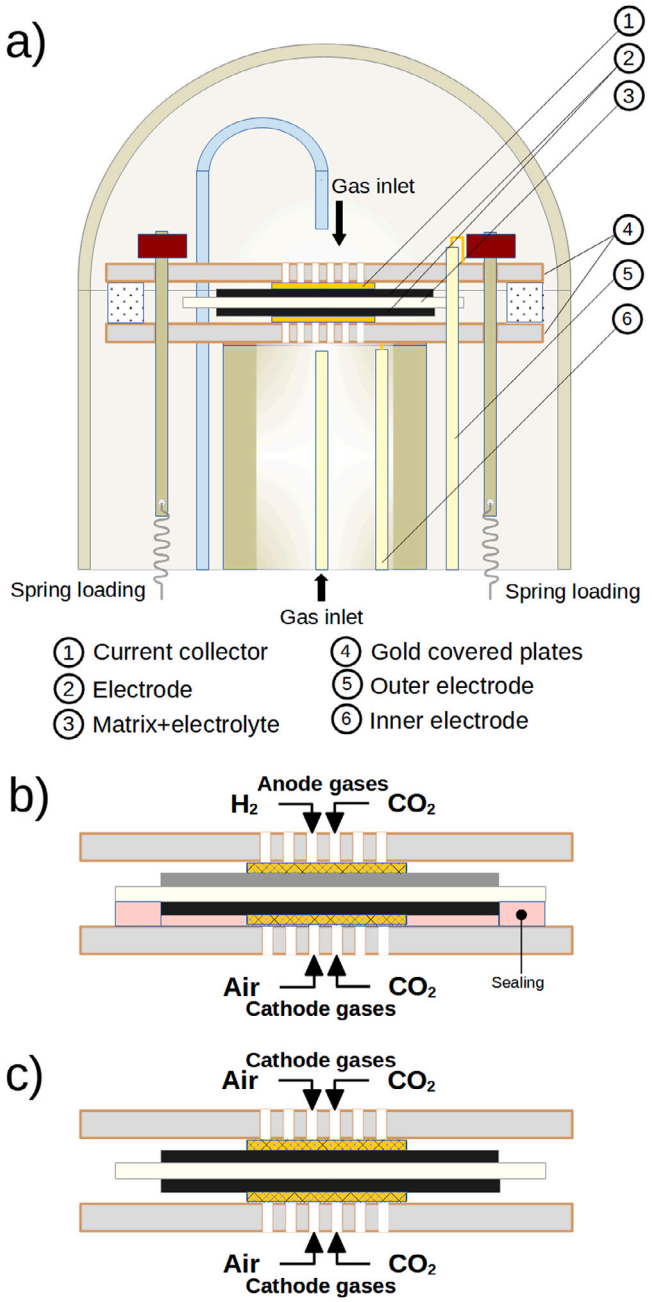

Fig. 2. Scheme of cell setup in the ProboStat sample holder (a); detailed cell configuration for single-cell performance test (b) and EIS measurements (c). (For interpretation of the references to color in this figure legend, the reader is referred to the web version of this article.)

650 °C. During the testing procedure fuel gas (H_2)80/(CO_2)20% and oxidant gas (air)70/(CO_2)30% were fed in, and reactant utilization factor was below 20%. Under the stable conditions, cell voltage and current were directly measured at the two electrodes. The single-cell testing materials and conditions are listed in Table 1. Cell voltage and current density were measured directly at the two electrodes. The performance of the cathode was evaluated based on the maximum power density (p_{max}) generated in each cell.

Cathode polarization and resistance characteristics were investigated by means of an electrochemical impedance spectroscopy (EIS). The circular-shaped cells were assembled in a symmetrical manner (cathodes on both sides) with an area of 1 cm^2 each, separated by the γ-$LiAlO_2$ matrix and $(Li_{0.62}/K_{0.38})_2CO_3$ electrolyte, and mounted in the ProboStat sample holder (setup depicted in Fig. 2a and c. Electrode current collectors (golden mesh) were adjacent to separator plates with gas channels (stainless steel covered with gold layer). Each plate was connected to electrode during the measurement. Analyzed cathodes were supplied with a gas flow rate identical to the cathodes used in the performance tests (see Table 2).

Measurements were performed for symmetrical single cells at open circuit voltage (OCV) using the GAMRY Reference 3000 potentiostat with the frequency ranging from 10^{-2} to 10^4 Hz at a temperature of 650 °C. Temperature control processes were conducted with use of the EUROTHERM 2408f controller. The gas mixtures applied during EIS measurements were composed of 10, 20 or 30% CO_2 corresponding to a partial pressure of pCO_2 = 0.1, 0.2 or 0.3 bar respectively, and various oxygen concentrations $\%O_2$ = 10, 15, 20 or 30% (pO_2 = 0.1, 0.15, 0.2 or 0.3 bar respectively). The mixtures were balanced by nitrogen to maintain the mass flow as in the performance test. The conditions of $\%O_2$ = 15% (pO_2 = 0.15 bar) and $\%CO_2$ = 30% (pO_2 = 0.3 bar) corresponds to the single-cell performance tests. The EIS results are indicated by semi-circles representing ohmic (R_o), charge transfer (R_{ct}) as well as mass transfer (R_{mt}) resistance related to specific frequency ranges. Based on the EIS analysis, polarization components such as internal ohmic resistance (R_o), charge transfer resistance (R_o), and mass transfer resistance (R_{mt}) were calculated from the equivalent circuit.

The equivalent circuit L × R_o(R_{ct}-CPE_{ct}) × (R_{mt}-CPE_{mt}), depicted in Fig. 7, contained an inductor L, representing the inductance of the cell and parasitic inductance of instrumentation and wiring, in series with a resistor R_o, representing ohmic resistance, in series with two parallel combinations of: resistor R_{ct} representing charge transfer resistance and a constant phase element CPE_{ct} corresponding to the surface roughness of porous electrodes and accounting for double layer capacitance, and a resistor R_{mt} representing mass transfer resistance and a constant phase element CPE_{mt} for the capacitance associated with a diffusion. This equivalent circuit is commonly chosen to represent the impedance behavior of the porous electrodes immersed in the molten carbonates [55,56].

3. Results and discussion

3.1. Microstructure characterization

The mean particle sizes of silver and nickel powders used for porous layers tape casting route were similar, approx. 8 and 12 μm, respectively, but the final microstructures of the silver and nickel oxide layers differ — see Fig. 3.

Due to lower melting point (≈962 °C) of silver, during the sintering process conducted at 800 °C, mass transport processes are more intensive than in the case of Ni (melting point ≈1455 °C), and consequently a lower porosity of the silver layer was obtained (Table 3).

3.2. Single-cell performance

The MCFC performance tests were carried out for single cells with the standard nickel oxide cathode, and new layered cathodes NA (NiO layer+Ag layer), NF (NiO layer+Ni foam layer), and NFA (NiO layer+Ni foam layer+Ag layer). During testing, the cathode was the only variable component, and the other materials (anode, matrix, electrolyte, current collectors), and conditions remained unchanged. As a result, the voltage–current density and power density-current density characteristics were obtained and presented in Fig. 4a and b, respectively.

The OCV values varied between the analyzed cathodes and for the N and NA are about 1 V which is the commonly achieved value for fuel cells, particularly MCFC, while for the NF cathode (1.21 V) they were higher, closer to theoretical value (1.23 V). The OCV obtained for the NFA (0.87 V) was the lowest amongst all analyzed cathodes but its decay was close to linear and not steep under loading which indicates better operational stability. Moreover, the NFA cathode generated

Table 2
Materials and operating conditions of single cells.

Cell component		Material	Area (cm^2)	Gas conditions	
Current collector		Gold wire mesh	1.0	–	
Cathode	N	NiO	1.0	Mole ratio of fuel gas (air:CO_2)	70:30
	NA	NiO + Ag		Total flow rate (cm^3 min^{-1})	50
	NF	NiO + Ni foam			
	NFA	NiO + Ni foam + Ag			
Electrolyte		$(Li_{0.62}/K_{0.38})_2CO_3$	n.a.	–	
Matrix		$LiAlO_2$	1.3	–	
Anode		Ni	1.0	Mole ratio of fuel gas (H_2:CO_2)	80:20
				Total flow rate (cm^3 min^{-1})	50
Current collector		Gold wire mesh	1.0	–	

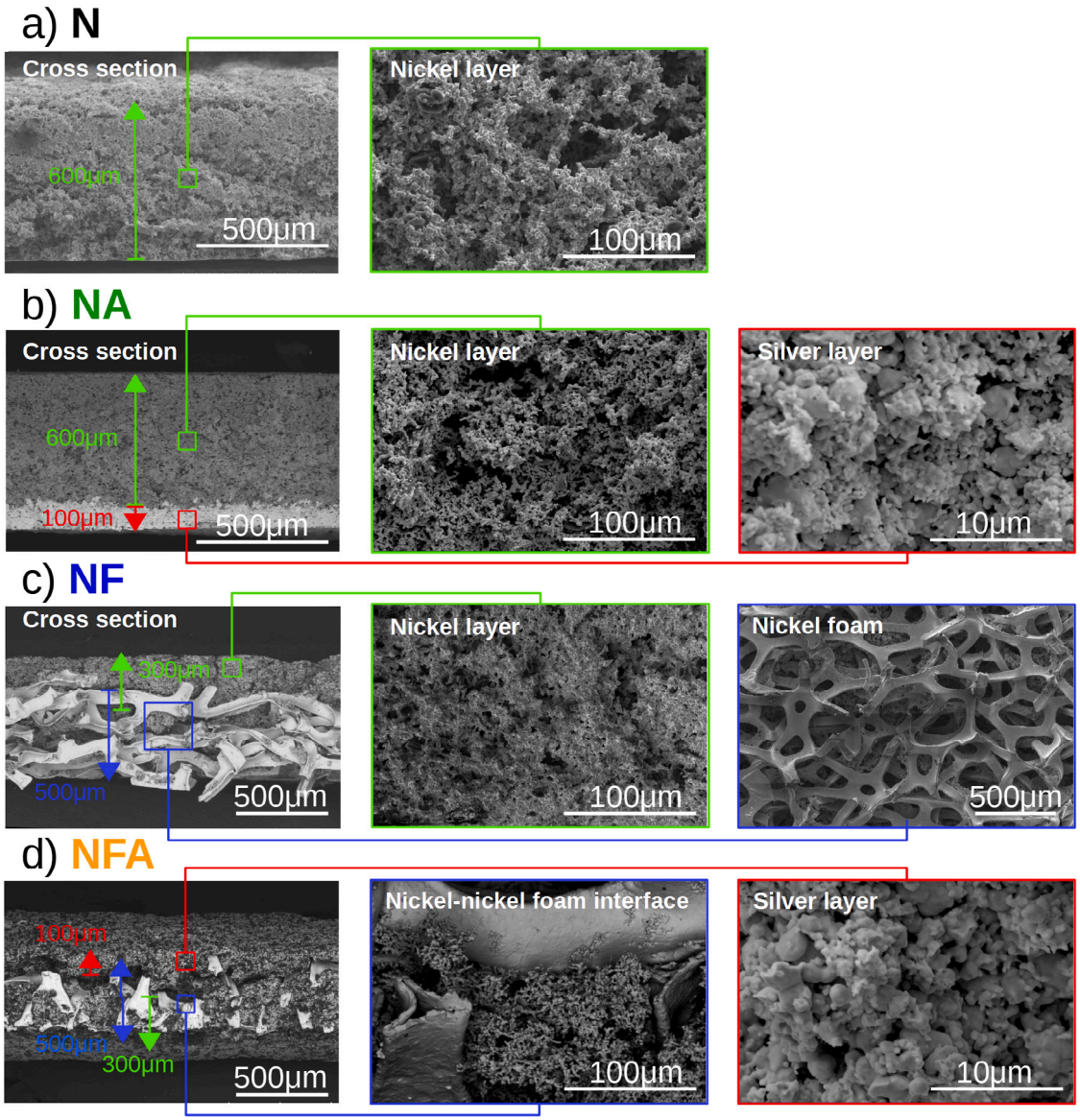

Fig. 3. Microstructure of the cathodes before operation (a) N, (b) NA, (c) NF, (d) NFA. (For interpretation of the references to colour in this figure legend, the reader is referred to the web version of this article.)

higher voltage above the current density of 0.4 A cm^{-2} in comparison to the other cathodes. In our studies, mica sealant was used which is a layered structure material and cannot ensure a perfect sealing. It can be concluded that the differences in OCV reflect how close the cell is to perfect sealing. The cells with NF and NFA cathodes achieved the highest and the lowest OCV thus it might be a reflection of their best and worst sealing, respectively. Even though the cell with the NFA cathode achieved the lowest OCV, it outperformed the other ones at high current density, which supports our conclusion of the best performance of the NFA cathode. Another reason may be the composition of the gas

Table 3
Porosity of cathode layers before operation.

Cathode	Layer	Porosity (%)
N	NiO	68.2
NA	NiO	69.8
	Ag	60.9
NF	NiO	68.8
	Ni foam	89.0
NFA	NiO	68.1
	Ni foam	89.0
	Ag	60.2

mixture at the anode side — consisting H_2 and CO_2. In such conditions the Ni anode can promote formation of CO and C, and in this case the OCV can be higher than 1 V (see [57]), unlike when only hydrogen is used. Commonly, the parameter used to describe the operational performance of electrodes is rather the maximum power density (p_{max}) reached under operation conditions. The maximum power density for MCFCs with cathodes N, NA, NF, and NFA were p_{max} = 151, 231, 231, and 249 mW cm^{-2} respectively (Fig. 4c). In order to better understand the extraordinary properties of the new cathodes, more extensive EIS studies have been performed, which enabled us to separate the contribution of electronic conductivity, charge transfer and gas diffusion to overall performance of MCFCs.

3.3. Electrochemical impedance spectroscopy measurements

The polarization of symmetric cells operated with analyzed cathodes were examined using electrochemical impedance spectroscopy (EIS) measurements. Generally, the impedance curve of porous electrodes contains two semi-circles (arcs): the high frequency arc related to charge-transfer resistance R_{ct} (electrode reaction kinetics) and the low frequency arc related to the mass-transfer resistance R_{mt} (gas diffusion in pore space or gas solubility and diffusion into molten carbonate electrolyte) [58]. The semi-circles may be overlapped in the frequency ranges in which certain processes with similar time constants have various contributions. The Nyquist plots show EIS data and the fitting for analyzed cathodes operated under different gas conditions — constant partial pressures of O_2 (various pCO_2; Fig. 5) or CO_2 (pO_2; Fig. 6) respectively. Three values of pCO_2 = 0.1, 0.2 or 0.3 bar, and four values of pO_2 = 0.1, 0.15, 0.2 or 0.3 bar were applied during the

Table 4
Quantification of cell resistance components (R_o, R_{ct} and R_{mt}) as a function of chemical composition of the cathode and composition of gas mixture (balanced by N_2).

Cathode	Gas mixture				Resistance components		
	$\%O_2$ (%)	pO_2 (bar)	$\%CO_2$ (%)	pCO_2 (bar)	R_o (Ω)	R_{ct} (Ω)	R_{mt} (Ω)
N (NiO)	10	0.1	10	0.1	0.90	4.64	7.94
			20	0.2	0.83	4.60	5.03
			30	0.3	0.78	4.19	4.10
	15	0.15	30	0.3	0.70	2.83	3.21
	20	0.2	10	0.1	0.64	2.16	3.43
			20	0.2	0.63	2.11	3.31
			30	0.3	0.62	2.10	3.22
	30	0.3	10	0.1	0.61	2.04	2.80
			20	0.2	0.58	1.91	2.74
			30	0.3	0.57	1.76	2.69
NA (NiO + Ag)	10	0.1	10	0.1	0.24	0.10	5.51
			20	0.2	0.22	0.08	5.38
			30	0.3	0.21	0.07	5.21
	15	0.15	30	0.3	0.21	0.07	4.15
	20	0.2	10	0.1	0.23	0.09	3.87
			20	0.2	0.22	0.08	3.73
			30	0.3	0.21	0.07	3.75
	30	0.3	10	0.1	0.23	0.10	3.27
			20	0.2	0.21	0.08	3.17
			30	0.3	0.20	0.07	3.08
NF (NiO + Ni foam)	10	0.1	10	0.1	0.20	0.09	4.03
			20	0.2	0.21	0.09	5.03
			30	0.3	0.20	0.07	5.97
	15	0.15	30	0.3	0.18	0.10	4.34
	20	0.2	10	0.1	0.15	0.13	3.00
			20	0.2	0.18	0.13	3.42
			30	0.3	0.20	0.07	4.24
	30	0.3	10	0.1	0.16	0.10	2.56
			20	0.2	0.18	0.08	2.66
			30	0.3	0.18	0.07	2.84
NFA (NiO + Ni foam + Ag)	10	0.1	10	0.1	0.14	0.46	0.73
			20	0.2	0.14	0.44	0.82
			30	0.3	0.14	0.39	0.81
	15	0.15	30	0.3	0.14	0.29	0.69
	20	0.2	10	0.1	0.13	0.36	0.52
			20	0.2	0.13	0.35	0.53
			30	0.3	0.13	0.32	0.61
	30	0.3	10	0.1	0.13	0.32	0.41
			20	0.2	0.13	0.24	0.44
			30	0.3	0.13	0.21	0.47

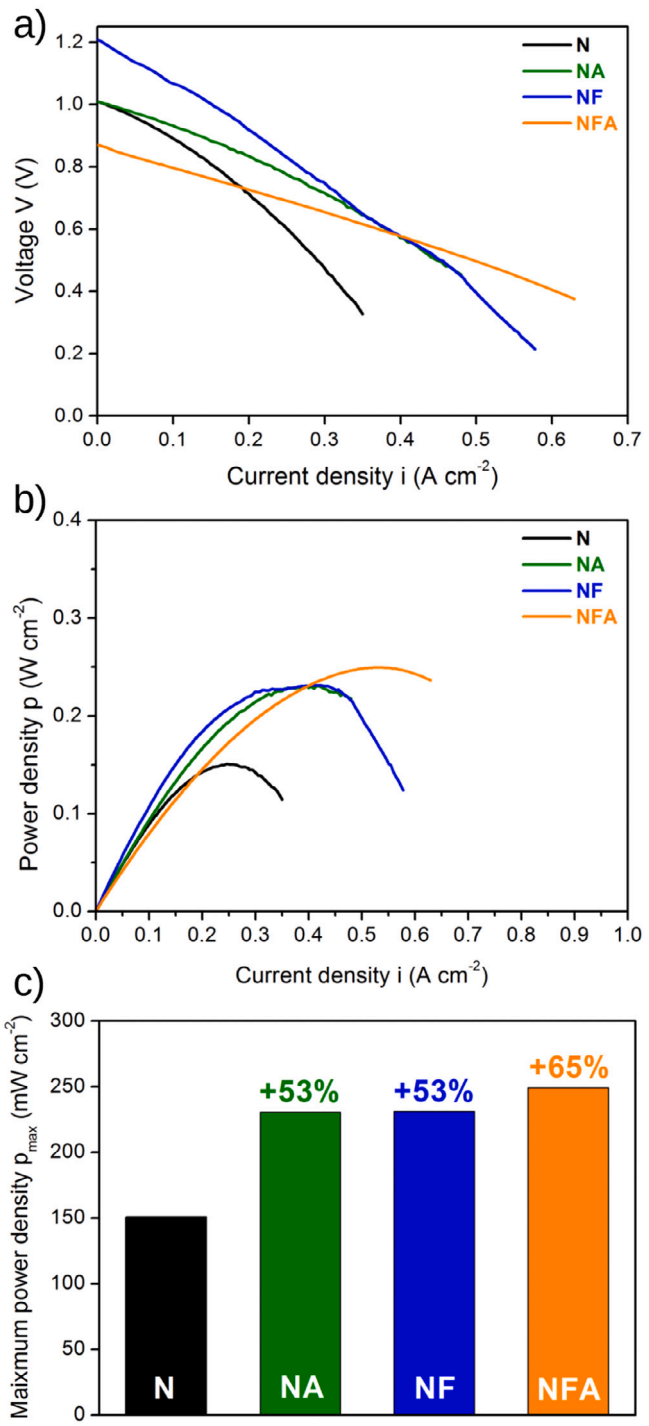

Fig. 4. Results of single-cell performance tests for the analyzed cathodes at operation temperature (650 °C): E-i curves (a), p-i curves (b). (For interpretation of the references to colour in this figure legend, the reader is referred to the web version of this article.)

measurements. The values of the resistance components, R_o, R_{ct} and R_{mt}, calculated after fitting to the equivalent circuit are summarized in Table 4 and depicted in Fig. 7.

The cell operated with commonly used MCFC cathode, herein N, composed of nickel (nickel oxide in operando) is a reference for other analyzed variants (NA, NF, NFA). Based on the Nyquist plots showing fitted EIS data – in Figs. 5 and 6 – it may be quantitatively inferred that: (i) all analyzed MCFC cathodes showed similar electrochemical behavior, (ii) the analyzed modifications of the cathode microstructure and chemical composition as well as varying gas conditions significantly affect the resistance components (R_o, R_{ct} and R_{mt}).

First, the influence of variation in CO_2 partial pressure will be discussed. Based on the EIS data in Fig. 5c,f,i,l it may be concluded that under pO_2 = 0.3 bar, the pCO_2 ranging from 0.1 to 0.3 bar does not affect the resistance behavior of cells operated with analyzed cathodes. The pCO_2 has clear impact on the impedance of N and NF cathodes under pO_2 = 0.1 bar (Fig. 5a and g, respectively) as well as NF cathode under pO_2 = 0.2 bar (Fig. 5h). In these cases, mass-transfer resistance components (R_{mt}) are significantly affected. For N cathode (nickel oxide), tested under pO_2 = 0.1 bar, all resistance components R_o, R_{ct} and R_{mt} decreases with increasing pCO_2. R_o dropped from 0.90 to 0.78 Ω, R_{ct} from 4.64 to 4.19 Ω, and R_{mt} from 7.94 to 4.10 Ω. For NF cathode (nickel oxide onto nickel foam layer), tested under pO_2 = 0.1 and 0.2 bar that relationship for R_{mt} is reverse — it increases (from 4.03 to 5.97 Ω and from 3.00 to 4.24 Ω respectively) with increasing pCO_2. Impedance spectra of cathodes denoted as NA (silver onto nickel oxide layer) and NFA (nickel oxide+nickel foam+silver layer) remain almost unaffected by the partial pressure of carbon dioxide.

The EIS results were also summarized in Fig. 6 to show the influence of various pO_2 on the resistance behavior of analyzed cathodes, when pCO_2 was kept constant at 0.1, 0.2, and 0.3 bar. This configuration of results renders possible the demonstration of significant dependence of the impedance on the partial pressure of oxygen for all cathodes. Internal ohmic resistance, R_o, calculated for NA, NF, and NFA cathodes have similar values for each pCO_2, is negligibly affected by the oxygen partial pressure variations. Moreover, the values of R_o components for NA, NF (both between 0.15 and 0.24 Ω), and for NFA (approx. 0.14 Ω) cathodes were up to 4 times lower than those calculated for N cathode (between 0.57 and 0.90 Ω). The substantial drops in R_o of N cathode can be observed between pO_2 = 0.1 and 0.2 bar (25–30%), and are larger than those between 0.2 and 0.3 bar. Thus, the cell operated with N cathode has distinctly higher resistance in oxygen lean gas mixtures (pO_2 = 0.1 bar). For all abovementioned gas conditions, the R_o components always reaches the lowest values for three layer electrode — NFA.

The conventional cathode (N) has similar charge-transfer and mass-transport resistance characteristics as for R_o resistance component. R_{ct} and R_{mt} also drops down substantially (over 50 and 25–50% respectively) between pO_2 = 0.1 and 0.2 bar, and the drops are larger than those between 0.2 and 0.3 bar. All calculated charge-transfer resistance components, R_{ct}, were substantially reduced for NA, NF, and NFA cathodes compared to the N one. At pO_2 = 0.1 bar, the reduction reaches even 40 times for NA as well as NF, and 10 times for NFA cathodes. In the case of R_{ct}, the lowest values were calculated for NA and NF, while the highest — for N conventional nickel oxide cathode. It can be noticed that mass-transport resistances, R_{mt}, calculated for the N and NA cathode are decreasing, and for the NF — increasing when partial pressure of carbon dioxide increases from 0.1 to 0.3 bar. The R_{mt} for the N, NA and NF cathodes are almost equal at pCO_2 = 0.2 bar in whole range of pO_2. When partial pressure of carbon dioxide is equal to 0.3 bar, the R_{mt} calculated for the N cathode is lower than those calculated for the NF and NA cathodes. For all analyzed gas conditions, in turn, mass-transport resistance components calculated for NFA cathode are the lowest and reduced substantially compared to the N, NA and NF cathodes.

4. Summary and conclusions

Summing up, conventional nickel oxide cathode (N) has the highest resistance among analyzed cathodes and achieved the lowest performance in operation conditions measured by the maximum power density (p_{max}). All resistance components are substantially lower for the higher partial pressure of oxygen, without being affected by the partial pressure of carbon dioxide to a similar extent. For the conventional cathode, made of nickel oxide, this effect might be attributed

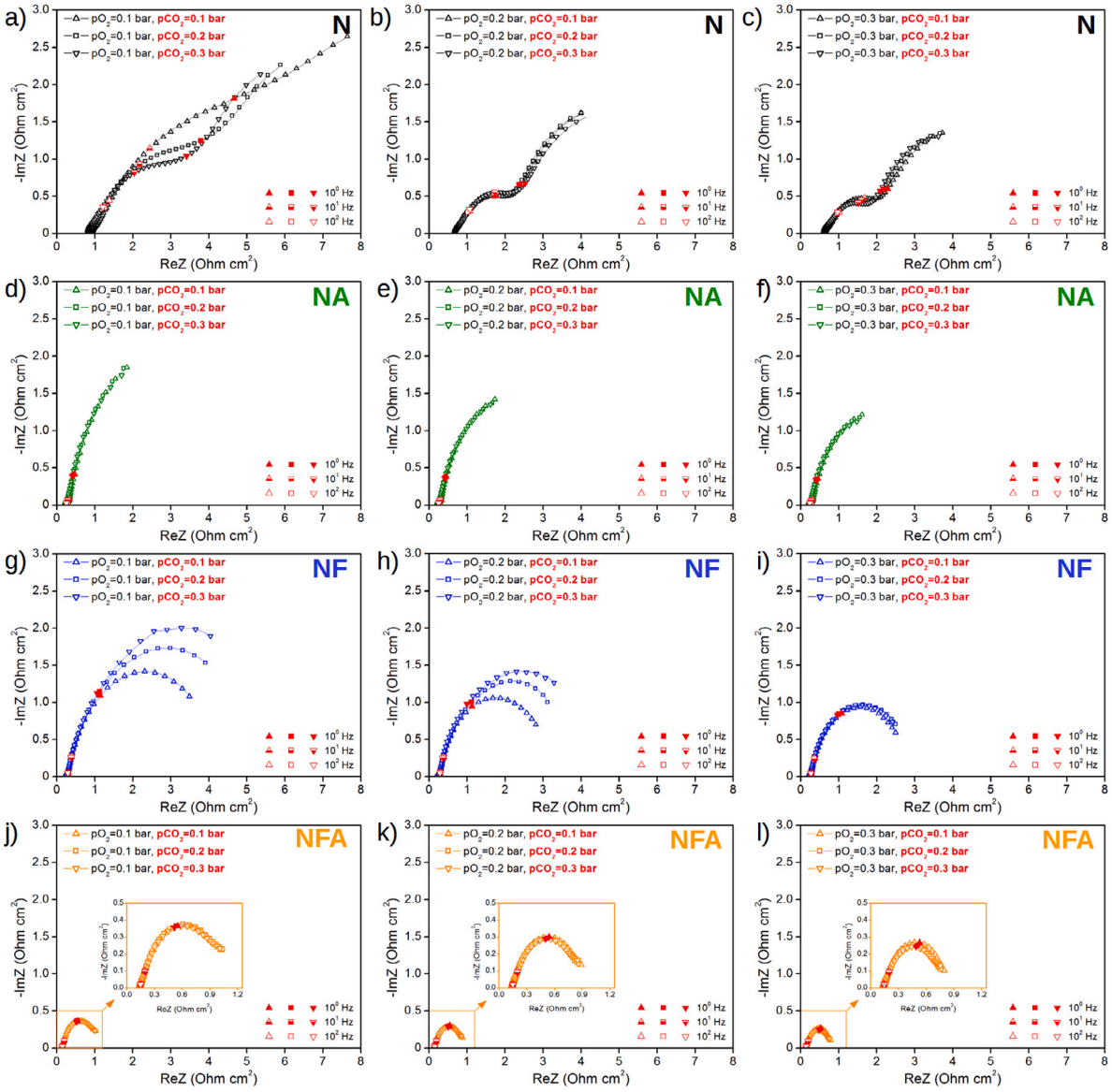

Fig. 5. EIS results for analyzed cathodes operated in symmetric cells at 650 °C under constant O_2 and various CO_2 partial pressures (pCO_2 = 0.1, 0.2, 0.3 bar). (For interpretation of the references to colour in this figure legend, the reader is referred to the web version of this article.)

to the oxygen reduction reaction. Therefore, it is considered as a rate determining step for the overall cathode reaction, it is promoted by the high oxygen partial pressure, and its activation energy decreases with increasing oxygen partial pressure [48,59–61].

The tape casting of the silver layer onto the nickel oxide layer (NA cathode) greatly reduces ohmic and charge-transfer resistance components comparing to the pure nickel oxide (N) cathode operated in analyzed gas conditions. Mass transport remains slightly affected, with the exception of pCO_2 = 0.1 bar and pO_2 = 0.1 bar. For this gas conditions, R_{mt} is reduced of approx. 25%. Moreover, the results of operation tests show that the presence of the tape cast silver layer in the cathode enhances MCFC performance. The reduction of R_{ct} may be attributed to lower contact resistance between the cathode and current collector after introducing the silver layer due to its very low resistivity (1.49×10^{-8} Ω m), and its stability in the oxidizing atmosphere as compared to nickel which is in situ oxidized and lithiated to $LiNiO_2$ during the cell operation [62,63]. The rate of the formation of the carbonate ion (CO_3^{2-}), via recombination of the activated oxygen and carbon dioxide, is also considered slow, and may be enhanced by Ag catalyst [64,65]. Thus, the NiO+Ag (NA) cathode can possibly operate well in oxygen-lean conditions — partial pressure of oxygen lower than 0.15 bar as it is commonly applied.

Cathode structure composed of conventional nickel oxide layer tape cast onto nickel foam (NF) also provides substantial reduction of ohmic resistance of the cell as well as charge transfer resistance compared to the pure nickel oxide (N) cathode. The behavior of NF cathode is comparable to NA in terms of performance (p_{max}) measured in single-cell tests as well as R_o and R_{ct} components in the whole range of applied partial pressures of oxygen and carbon dioxide. Low internal resistance of the cell may result from the high electrical conductivity of nickel foam layer adjacent to current collectors and its lower susceptibility to in situ oxidation than the porous sinter made of fine nickel powder. Large pores in the foam layer (50 to 250 μm in diameter) are not soaked by the molten electrolyte so they remain permeable for gases which can be delivered sufficiently to the active reaction sites in the nickel oxide layer (triple phase boundaries). Surprisingly, the mass-transport resistance is growing for the NF cathode with increasing partial pressure of carbon dioxide what is an opposite effect to the other cathodes. Higher resistance of the cathode may result from the negative order of the oxygen reduction reaction in MCFC for carbon dioxide and,

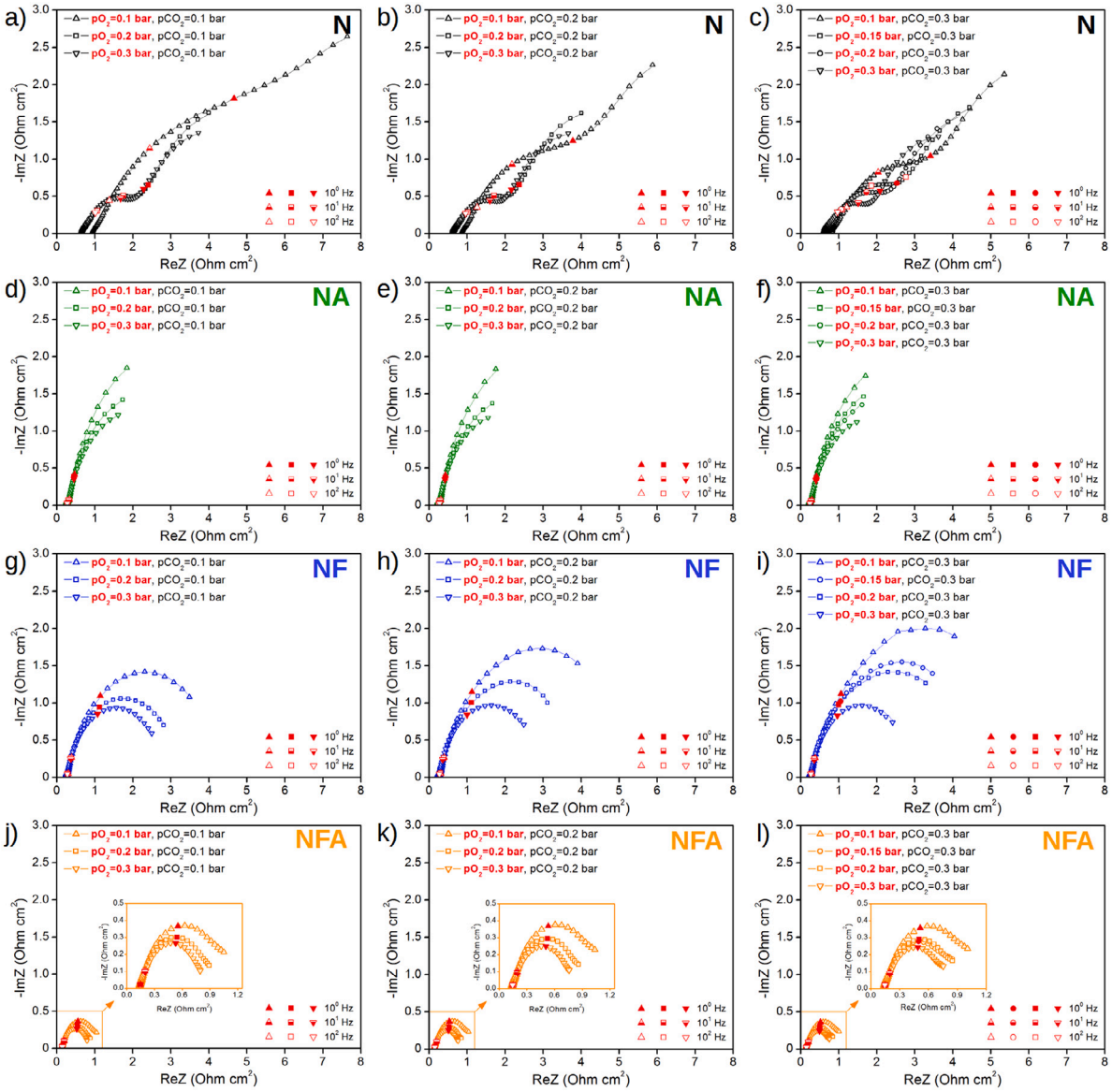

Fig. 6. EIS results for analyzed cathodes operated in symmetric cells at 650 °C under constant CO_2 and various O_2 partial pressures (pO_2 = 0.1, 0.2, 0.3 bar). (For interpretation of the references to colour in this figure legend, the reader is referred to the web version of this article.)

therefore, from its dependence on gas partial pressure. Oxide formation, oxygen reduction and carbonate ion formation are promoted by the high oxygen partial pressure and low carbon dioxide partial pressure. During the performance tests, NF cathode achieved the same maximum power density as the NA cathode.

The NFA cathode constitutes a conjunction of all positive characteristics of NA and NF cathodes. All calculated resistance components are greatly reduced compared to the conventional nickel oxide cathode (N), and beside R_{ct} the lowest for all gas conditions. Nevertheless, the R_{ct} of the NFA cathode is still very similar to the NA and NF. Also, the maximum power density measured in the operation conditions is the highest for the NFA cathode. Therefore, the NFA cathode combines improved electrical conductivity and lower contact resistance (Ag layer), permeability for gases (nickel foam layer), high catalytic activity (Ag and NiO layers), and sufficient interaction with the electrolyte (NiO layer).

General trends in layered electrode development may be distinguished also for SOFCs [66–68]. Particular layers are introduced mainly for improvement of current collection, ionic/electronic conductivity or compatibility with the electrolyte. Bi-layered $LaMnO_3/Co_3O_4$ coating electrodeposited on metallic wire network [69] has been reported as improving the power density and durability of a tubular SOFC by stabilizing the surface of the metallic wire network used as a cathode current collector. Layers designed for facile mixed ionic/electronic conduction are commonly composed of a mixture of Ni(O) and ion conductive ceramics like LSM, LSCo or YSZ [66,70] or CGO [71]. To substantially reduce the cell degradation in electrolysis mode and avoid the electrode delamination, ScSZ (Sc_2O_3 stabilized ZrO_2) interlayer on the cathode side was introduced [71]. As it may be inferred based on the recent literature reports, the main goal for SOFCs is particularly lowering the operation temperature to intermediate temperatures – IT-SOFCs or increasing stability in electrolysis mode, while for MCFCs – improvement of the power density up to SOFC level. These similarities in electrode design for MCFCs and SOFCs are inspiring and appear to reflect the mutual goals to develop hybrid MCFC–SOFC solutions.

CRediT authorship contribution statement

K. Ćwieka: Methodology, Investigation, Data curation, Writing - original draft, Review & editing, Visualization. **A. Lysik:** Investigation,

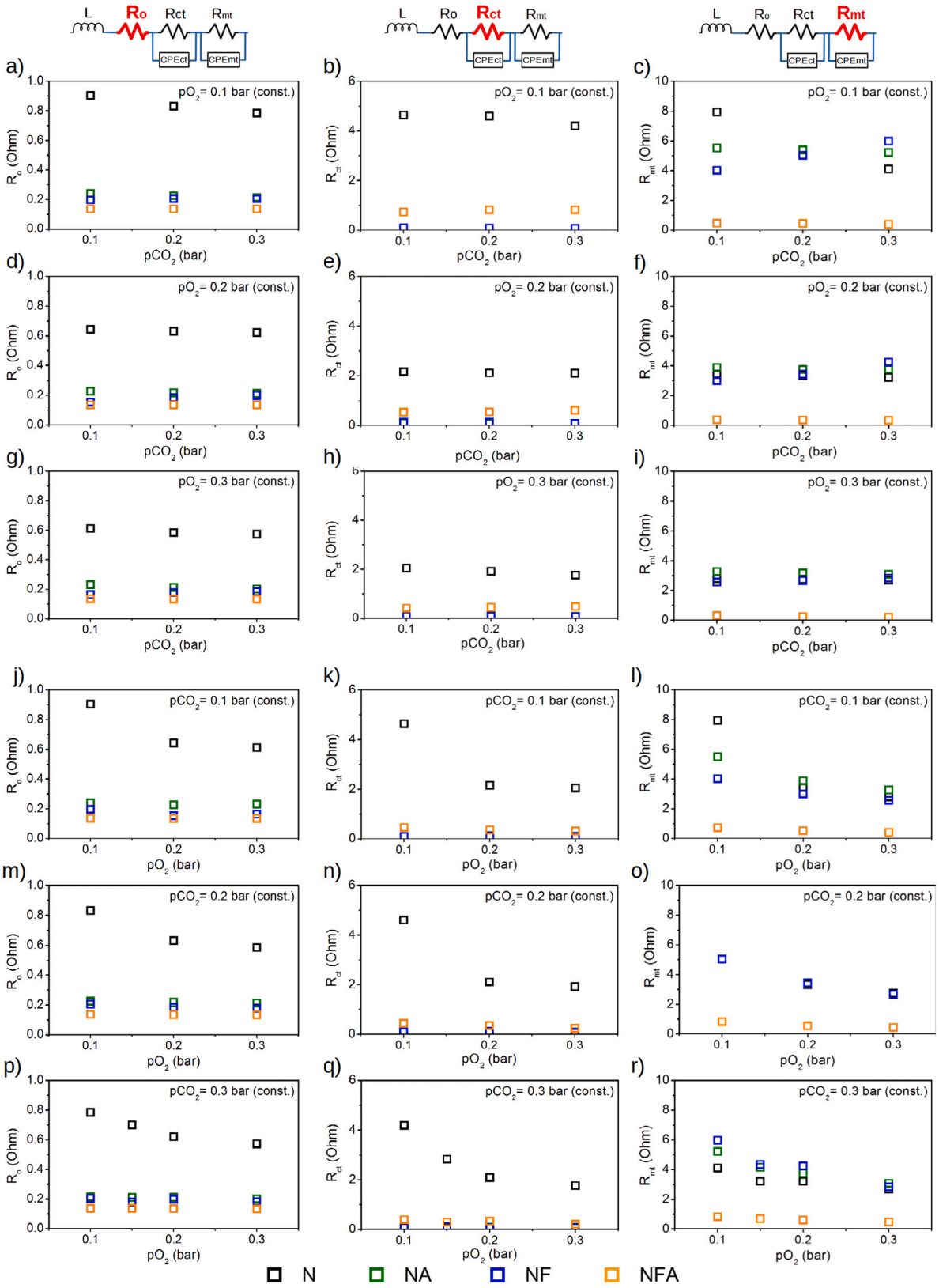

Fig. 7. Comparison of ohmic (R_o), charge-transfer (R_{ct}), and mass-transfer (R_{mt}) resistances of analyzed cathodes operated at 650 °C under (a-i) constant O_2 and various pCO_2 and (j-r) constant CO_2 and various pO_2. (For interpretation of the references to colour in this figure legend, the reader is referred to the web version of this article.)

Data Curation. **T. Wejrzanowski:** Conceptualization, Resources, Supervision, Project administration, Funding acquisition. **T. Norby:** Writing - review & editing. **W. Xing:** Methodology, Investigation, Supervision, Project administration, Funding acquisition.

Declaration of competing interest

The authors declare that they have no known competing financial interests or personal relationships that could have appeared to influence the work reported in this paper.

Acknowledgments

This work was financially supported by the Polish National Science Center in the framework of the OPUS research project (Grant No. 2017/27/B/ST8/02763) and the National Center for Research and Development, Poland under contract No. M-ERA.NET2/2016/04/2017.

References

[1] P. Tomczyk, MCFC Versus other fuel cells-characteristics, technologies and prospects, J. Power Sources 160 (2) (2006) 858–862, http://dx.doi.org/10.1016/j.jpowsour.2006.04.071.

[2] Fuel cells – molten carbonate fuel cells - overview, in: Encyclopedia of Electrochemical Power Sources, 2009, pp. 446–453, http://dx.doi.org/10.1016/b978-044452745-5.00263-x.

[3] K. Sundmacher, Fuel cell engineering: Toward the design of efficient electrochemical power plants, Ind. Eng. Chem. Res. 49 (21) (2010) 10159–10182, http://dx.doi.org/10.1021/ie100902t.

[4] M. Cassir, S. McPhail, A. Moreno, Strategies and new developments in the field of molten carbonates and high-temperature fuel cells in the carbon cycle, Int. J. Hydrogen Energy 37 (24) (2012) 19345–19350, http://dx.doi.org/10.1016/j.ijhydene.2011.11.006, 2011 International Workshop on Molten Carbonates & Related Topics.

[5] J.R. Selman, C.C. Chen, Scientific and technical maturity of molten carbonate technology, Int. J. Hydrogen Energy 37 (24) (2012) 19280–19288, http://dx.doi.org/10.1016/j.ijhydene.2012.06.016.

[6] S. Abate, G. Centi, S. Perathoner, Energy-related catalysis, Natl. Sci. Rev. 2 (2) (2015) 143–145, http://dx.doi.org/10.1093/nsr/nwv017.

[7] J. Molenda, J. Kupecki, R. Baron, M. Blesznowski, G. Brus, T. Brylewski, M. Bucko, J. Chmielowiec, K. Cwieka, M. Gazda, A. Gil, P. Jasinski, Z. Jaworski, J. Karczewski, M. Kawalec, R. Kluczowski, M. Krauz, F. Krok, B. Lukasik, M. Malys, A. Mazur, A. Mielewczyk-Gryn, J. Milewski, S. Molin, G. Mordarski, M. Mosialek, K. Motylinski, E.N. Naumovich, P. Nowak, G. Pasciak, P. Pianko-Oprych, D. Pomykalska, M. Rekas, A. Sciazko, K. Swierczek, J. Szmyd, S. Wachowski, T. Wejrzanowski, W. Wrobel, K. Zagorski, W. Zajac, A. Zurawska, Status report on high temperature fuel cells in Poland - recent advances and achievements, Int. J. Hydrogen Energy 42 (2017) 4366–4403, http://dx.doi.org/10.1016/j.ijhydene.2016.12.087.

[8] R. Bove, P. Lunghi, Experimental comparison of MCFC performance using three different biogas types and methane, J. Power Sources 145 (2) (2005) 588–593, http://dx.doi.org/10.1016/j.jpowsour.2005.01.069.

[9] T. Watanabe, Y. Izaki, Y. Mugikura, H. Morita, M. Yoshikawa, M. Kawase, F. Yoshiba, K. Asano, Applicability of molten carbonate fuel cells to various fuels, J. Power Sources 160 (2) (2006) 868–871, http://dx.doi.org/10.1016/j.jpowsour.2006.06.058.

[10] S. Erzen, E. Açıkkalp, A. Hepbasli, Performance assessment of a biogas fuelled molten carbonate fuel cell-thermophotovoltaic cell-thermally regenerative electrochemical cycle-absorption refrigerator-alkaline electrolyzer for multigenerational applications, Int. J. Hydrogen Energy 44 (42) (2019) 23741–23749, http://dx.doi.org/10.1016/j.ijhydene.2019.07.057.

[11] G. Centi, S. Perathoner, Catalysis: Role and challenges for a sustainable energy, Top. Catalysis 52 (8) (2009) 948–961, http://dx.doi.org/10.1007/s11244-009-9245-x.

[12] L. Caprile, B. Passalacqua, A. Torazza, Carbon capture: Energy wasting technologies or the MCFCs challenge?, Int. J. Hydrogen Energy 36 (16) (2011) 10269–10277, http://dx.doi.org/10.1016/j.ijhydene.2010.10.028.

[13] A. Kulkarni, S. Giddey, Materials issues and recent developments in molten carbonate fuel cells, J. Solid State Electrochem. 16 (2012) 3123–3146, http://dx.doi.org/10.1007/s10008-012-1771-y.

[14] K. Czelej, K. Cwieka, J. Colmenares, K. Kurzydlowski, Atomistic insight into the electrode reaction mechanism of the cathode in molten carbonate fuel cells, J. Mater. Chem. A 5 (26) (2017) http://dx.doi.org/10.1039/c7ta02011b.

[15] K. Czelej, K. Cwieka, J. Colmenares, K. Kurzydlowski, Catalytic activity of nio cathode in molten carbonate fuel cells, Appl. Catal. B 222 (2018) http://dx.doi.org/10.1016/j.apcatb.2017.10.003.

[16] T. Wejrzanowski, S.H. Ibrahim, K. Cwieka, J. Milewski, K.J. Kurzydlowski, Design of open-porous materials for high-temperature fuel cells, J. Power Technol. 96 (3) (2016) 178–182.

[17] T. Wejrzanowski, S. Haj Ibrahim, K. Cwieka, M. Loeffler, J. Milewski, E. Zschech, C.-G. Lee, Multi-modal porous microstructure for high temperature fuel cell application, J. Power Sources 373 (2018) http://dx.doi.org/10.1016/j.jpowsour.2017.11.009.

[18] R. Baron, T. Wejrzanowski, J. Milewski, Ł. Szabłowski, A. Szczęśniak, K.-Z. Fung, Manufacturing of γ-lialo$_2$ matrix for molten carbonate fuel cell by high-energy milling, Int. J. Hydrogen Energy 43 (13) (2018) 6696–6700, http://dx.doi.org/10.1016/J.IJHYDENE.2018.02.085.

[19] N.P. Brandon, D.J. Brett, Engineering porous materials for fuel cell applications., Philos. Trans. Ser. A Math. Phys. Eng. Sci. 364 (1838) (2006) 147–159, http://dx.doi.org/10.1098/rsta.2005.1684.

[20] R. O'Hayre, D.M. Barnett, F.B. Prinz, The triple phase boundary. a mathematical model and experimental investigations for fuel cells, J. Electrochem. Soc. 152 (2) (2005) A439–A444, http://dx.doi.org/10.1149/1.1851054.

[21] B. Kenney, M. Valdmanis, C. Baker, J. Pharoah, K. Karan, Computation of TPB length, surface area and pore size from numerical reconstruction of composite solid oxide fuel cell electrodes, J. Power Sources 189 (2) (2009) 1051–1059, http://dx.doi.org/10.1016/j.jpowsour.2008.12.145.

[22] J.D. Fehribach, R. O'Hayre, Triple phase boundaries in solid-oxide cathodes, SIAM J. Appl. Math. 70 (2) (2009) 510–530, http://dx.doi.org/10.1137/080722667.

[23] A. Wijayasinghe, B. Bergman, C. Lagergren, A study on $LiCoO_2$-rich cathode materials for the MCFC based on the $LiCoO_2$-$LiFeO_2$-NiO ternary system, Electrochim. Acta 49 (26) (2004) 4709–4717, http://dx.doi.org/10.1016/j.electacta.2004.05.026.

[24] J. Skibinski, K. Cwieka, T. Kowalkowski, B. Wysocki, T. Wejrzanowski, K.J. Kurzydlowski, The influence of pore size variation on the pressure drop in open-cell foams, Mater. Des. 87 (2015) 650–655, http://dx.doi.org/10.1016/j.matdes.2015.08.079.

[25] D. Westhoff, J. Skibinski, O. Šedivý, B. Wysocki, T. Wejrzanowski, V. Schmidt, Investigation of the relationship between morphology and permeability for open-cell foams using virtual materials testing, Mater. Des. 147 (2018) 1–10, http://dx.doi.org/10.1016/J.MATDES.2018.03.022.

[26] S. Haj Ibrahim, J. Skibinski, G. Oliver, T. Wejrzanowski, Microstructure effect on the permeability of the tape-cast open-porous materials, Mater. Des. 167 (2019) 107639, http://dx.doi.org/10.1016/J.MATDES.2019.107639.

[27] T. Wejrzanowski, J. Gluch, S. Ibrahim, K. Cwieka, J. Milewski, E. Zschech, Characterization of spatial distribution of electrolyte in molten carbonate fuel cell cathodes, Adv. Energy Mater. 20 (6) (2018) http://dx.doi.org/10.1002/adem.201700909.

[28] T. Wejrzanowski, K. Cwieka, J. Skibinski, A. Lysik, S.H. Ibrahim, J. Milewski, W. Xing, C.-G. Lee, Microstructure driven design of porous electrodes for molten carbonate fuel cell application: Recent progress, Int. J. Hydrogen Energy (2019) http://dx.doi.org/10.1016/J.IJHYDENE.2019.12.038.

[29] G. Gaiselmann, M. Neumann, V. Schmidt, O. Pecho, T. Hocker, L. Holzer, Quantitative relationships between microstructure and effective transport properties based on virtual materials testing, AIChE J. 60 (6) (2014) 1983–1999, http://dx.doi.org/10.1002/aic.14416.

[30] S. Haj Ibrahim, M. Neumann, F. Klingner, V. Schmidt, T. Wejrzanowski, Analysis of the 3D microstructure of tape-cast open-porous materials via a combination of experiments and modeling, Mater. Des. 133 (2017) 216–223, http://dx.doi.org/10.1016/j.matdes.2017.07.058.

[31] H. Moussaoui, R. Sharma, J. Debayle, Y. Gavet, G. Delette, J. Laurencin, Microstructural correlations for specific surface area and triple phase boundary length for composite electrodes of solid oxide cells, J. Power Sources 412 (2019) 736–748, http://dx.doi.org/10.1016/J.JPOWSOUR.2018.11.095.

[32] S. Haj Ibrahim, T. Wejrzanowski, P. Sobczak, K. Cwieka, A. Lysik, J. Skibinski, G.J. Oliver, Insight into cathode microstructure effect on the performance of molten carbonate fuel cell, J. Power Sources 491 (2021) 229562, http://dx.doi.org/10.1016/j.jpowsour.2021.229562.

[33] T. Wejrzanowski, K. Cwieka, J. Skibinski, T. Brynk, S.H. Ibrahim, J. Milewski, W. Xing, Metallic foam supported electrodes for molten carbonate fuel cells, Mater. Des. 193 (2020) 108864, http://dx.doi.org/10.1016/j.matdes.2020.108864.

[34] E. Antolini, The stability of molten carbonate fuel cell electrodes: A review of recent improvements, Appl. Energy 88 (12) (2011) 4274–4293, http://dx.doi.org/10.1016/j.apenergy.2011.07.009.

[35] B. Huang, F. Li, Q.-C. Yu, G. Chen, B.-Y. Zhao, K.-A. Hu, Study of nio cathode modified by zno additive for MCFC, J. Power Sources 128 (2004) 135–144, http://dx.doi.org/10.1016/j.jpowsour.2003.10.008.

[36] B. Huang, G. Chen, F. Li, Q.C. Yu, K.A. Hu, Study of nio cathode modified by rare earth oxide additive for MCFC by electrochemical impedance spectroscopy, Electrochim. Acta 49 (28) (2004) 5055–5068, http://dx.doi.org/10.1016/j.electacta.2004.04.019.

[37] B. Huang, Q.-c. Yu, H.-m. Wang, G. Chen, K.-a. Hu, Study of lifeo$_2$ coated nio as cathodes for MCFC by electrochemical impedance spectroscopy, J. Power Sources 137 (2) (2004) 163–174, http://dx.doi.org/10.1016/j.jpowsour.2004.05.015.

[38] M.Z. Hong, H.S. Lee, M.H. Kim, E.J. Park, H.W. Ha, K. Kim, TiO_2 - Coated Ni powder as a new cathode material for molten carbonate fuel cells, J. Power Sources 156 (2) (2006) 158–165, http://dx.doi.org/10.1016/j.jpowsour.2005.03.236.

[39] S.A. Song, S.C. Jang, J. Han, S.P. Yoon, S.W. Nam, I.H. Oh, S.G. Oh, Electrode performance of a new $La_{0.6}Sr_{0.4}Co_{0.2}Fe_{0.8}O_3$ coated cathode for molten carbonate fuel cells, Int. J. Hydrogen Energy 37 (24) (2012) 19304–19311, http://dx.doi.org/10.1016/j.ijhydene.2012.04.081.

[40] S.A. Song, H.T. Kim, K. Kim, S.N. Lim, S.P. Yoon, S.-C. Jang, Effect of LiNiO2-coated cathode on cell performance in molten carbonate fuel cells, Int. J. Hydrogen Energy 44 (23) (2019) 12085–12093, http://dx.doi.org/10.1016/J.IJHYDENE.2019.03.080.

[41] V.A. Lavrenko, A.I. Malyshevskaya, L.I. Kuznetsova, V.F. Litvinenko, V.N. Pavlikov, Features of high-temperature oxidation in air of silver and alloy Ag-Cu, and adsorption of oxygen on silver, Powder Metall. Metal Ceram. 45 (9–10) (2006) 476–480, http://dx.doi.org/10.1007/s11106-006-0108-8.

[42] H. Erikson, A. Sarapuu, K. Tammeveski, Oxygen reduction reaction on silver catalysts in alkaline media: a minireview, ChemElectroChem 6 (1) (2019) 73–86, http://dx.doi.org/10.1002/celc.201800913.

[43] I. Trachtenberg, Polarization studies of molten carbonate fuel cell electrodes, J. Electrochem. Soc. 111 (1) (1964) 110–113, http://dx.doi.org/10.1149/1.2426044.

[44] V.D. Belyaev, V.A. Sobyanin, V.N. Parmon, S. Freni, M. Aquino, Oxidative Conversion of CH_4 on Ni and Ag Electrode-Catalysts in Molten Carbonate Fuel Cell Reactor, Tech. Rep., 1993.

[45] K.T. Lee, A. Manthiram, Electrochemical performance of $Nd_{0.6}Sr_{0.4}Co_{0.5}Fe_{0.5}?ø_{3-\delta}$-Ag composite cathodes in intermediate temperature solid oxide fuel cells, J. Power Sources 160 (2 SPEC. ISS.) (2006) 903–908, http://dx.doi.org/10.1016/j.jpowsour.2006.02.027.

[46] T.J. Huang, X.D. Shen, C.L. Chou, Characterization of cu, ag and pt added $La_{0.6}Sr_{0.4}Co_{0.2}Fe_{0.8}O_{3-\delta}$ and gadolinia-doped ceria as solid oxide fuel cell electrodes by temperature-programmed techniques, J. Power Sources 187 (2) (2009) 348–355, http://dx.doi.org/10.1016/j.jpowsour.2008.11.019.

[47] T. Wu, Y. Rao, R. Peng, C. Xia, Fabrication and evaluation of ag-impregnated $bace_{0.8}sm_{0.2}o_{2.9}$ composite cathodes for proton conducting solid oxide fuel cells, J. Power Sources 195 (17) (2010) 5508–5513, http://dx.doi.org/10.1016/j.jpowsour.2010.03.063.

[48] S.A. Song, M.G. Kang, J. Han, S.P. Yoon, S.W. Nam, I.H. Oh, D.K. Choi, An ag-coated nio cathode for MCFCs operating at low temperatures, J. Electrochem. Soc. 158 (6) (2011) B660, http://dx.doi.org/10.1149/1.3571532.

[49] A. Lysik, K. Cwieka, T. Wejrzanowski, J. Skibinski, J. Milewski, F.M. Marques, T. Norby, W. Xing, Silver coated cathode for molten carbonate fuel cells, Int. J. Hydrogen Energy 45 (38) (2020) 19847–19857, http://dx.doi.org/10.1016/j.ijhydene.2020.05.112.

[50] B.-A. Mei, J. Lau, T. Lin, S.H. Tolbert, B.S. Dunn, L. Pilon, Physical interpretations of electrochemical impedance spectroscopy of redox active electrodes for electrical energy storage, J. Phys. Chem. C 122 (43) (2018) 24499–24511, http://dx.doi.org/10.1021/acs.jpcc.8b05241.

[51] J. Nielsen, J. Hjelm, Impedance of SOFC electrodes: A review and a comprehensive case study on the impedance of lsm:ysz cathodes, Electrochim. Acta 115 (2014) 31–45, http://dx.doi.org/10.1016/j.electacta.2013.10.053.

[52] A. Flura, C. Nicollet, S. Fourcade, V. Vibhu, A. Rougier, J.-M. Bassat, J.-C. Grenier, Identification and modelling of the oxygen gas diffusion impedance in sofc porous electrodes: application to pr2nio4+δ, Electrochim. Acta 174 (2015) 1030–1040, http://dx.doi.org/10.1016/j.electacta.2015.06.084.

[53] C. Endler-Schuck, J. Joos, C. Niedrig, A. Weber, E. Ivers-Tiffée, The chemical oxygen surface exchange and bulk diffusion coefficient determined by impedance spectroscopy of porous La0.58Sr0.4Co0.2Fe0.8O3 δ (LSCF) cathodes, Solid State Ion. 269 (2015) 67–79, http://dx.doi.org/10.1016/j.ssi.2014.11.018.

[54] E. Audasso, L. Barelli, G. Bidini, B. Bosio, G. Discepoli, Molten carbonate fuel cell performance analysis varying cathode operating conditions for carbon capture applications, J. Power Sources 348 (2017) 118–129, http://dx.doi.org/10.1016/j.jpowsour.2017.02.081.

[55] A. Meléndez-Ceballos, V. Albin, C. Crapart, V. Lair, A. Ringuedé, M. Cassir, Influence of cs and rb additions in lik and lina molten carbonates on the behaviour of MCFC commercial porous Ni cathode, Int. J. Hydrogen Energy 42 (3) (2017) 1853–1858, http://dx.doi.org/10.1016/J.IJHYDENE.2016.09.118.

[56] G. Accardo, D. Frattini, S.P. Yoon, H.C. Ham, S.W. Nam, Performance and properties of anodes reinforced with metal oxide nanoparticles for molten carbonate fuel cells, J. Power Sources 370 (2017) 52–60, http://dx.doi.org/10.1016/j.jpowsour.2017.10.015.

[57] Y. Nabae, K.D. Pointon, J.T.S. Irvine, Ni/c slurries based on molten carbonates as a fuel for hybrid direct carbon fuel cells, J. Electrochem. Soc. 156 (6) (2009) B716, http://dx.doi.org/10.1149/1.3110862.

[58] L. Giorgi, M. Carewska, S. Scaccia, E. Simonetti, E. Giacometti, R. Tulli, Development of molten carbonate fuel cell using novel cathode material, Int. J. Hydrogen Energy 21 (6) (1996) 491–496, http://dx.doi.org/10.1016/0360-3199(95)00097-6.

[59] C.Y. Yuh, J.R. Selman, The polarization of molten carbonate fuel cell electrodes, J. Electrochem. Soc. 138 (12) (1991) 3642, http://dx.doi.org/10.1149/1.2085473.

[60] K. Janowitz, M. Kah, H. Wendt, Molten carbonate fuel cell research: Part I. Comparing cathodic oxygen reduction in lithium/potassium and lithium/sodium carbonate melts, Electrochim. Acta 45 (7) (1999) 1025–1037, http://dx.doi.org/10.1016/S0013-4686(99)00305-9.

[61] J. Milewski, G. Discepoli, U. Desideri, Modeling the performance of MCFC for various fuel and oxidant compositions, Int. J. Hydrogen Energy 39 (22) (2014) 11713–11721, http://dx.doi.org/10.1016/J.IJHYDENE.2014.05.151.

[62] F. Pérez, D. Duday, M. Hierro, C. Gómez, M. Romero, M. Casais, J. Alonso, M. Martınez, L. Daza, Analysis by electrochemical impedance spectroscopy of new MCFC cathode materials, J. Power Sources 86 (1–2) (2000) 309–315, http://dx.doi.org/10.1016/S0378-7753(99)00422-X.

[63] J. Molenda, P. Wilk, J. Marzec, Structural, electrical and electrochemical properties of $LiNiO_2$, Solid State Ion. 146 (1–2) (2002) 73–79, http://dx.doi.org/10.1016/S0167-2738(01)00992-4.

[64] I. Stensgaard, E. Laegsgaard, F. Besenbacher, The reaction of carbon dioxide with an oxygen precovered ag(110) surface, J. Chem. Phys. 103 (22) (1995) 9825–9831, http://dx.doi.org/10.1063/1.469949.

[65] V. Nekrasov, A. Lystsov, O. Limanovskaya, N. Batalov, M. Konopelko, Oxygen reduction on gold electrode in Li_2CO_3 / K_2CO_3 (62 / 38 mol %) molten electrolyte: experimental and simulation analysis, Electrochim. Acta 182 (2015) 61–66, http://dx.doi.org/10.1016/J.ELECTACTA.2015.09.043.

[66] P. Holtappels, C. Bagger, Fabrication and performance of advanced multi-layer sofc cathodes, J. Eur. Ceram. Soc. 22 (1) (2002) 41–48, http://dx.doi.org/10.1016/S0955-2219(01)00238-2.

[67] W.H. Kan, A.J. Samson, V. Thangadurai, Trends in electrode development for next generation solid oxide fuel cells, J. Mater. Chem. A 4 (2016) 17913–17932, http://dx.doi.org/10.1039/C6TA06757C.

[68] S. Hussain, L. Yangping, Review of solid oxide fuel cell materials: cathode, anode, and electrolyte, Energy Transit. 4 (2) (2020) 113–126, http://dx.doi.org/10.1007/s41825-020-00029-8.

[69] B.-K. Park, R.-H. Song, S.-B. Lee, T.-H. Lim, S.-J. Park, W. Jung, J.-W. Lee, Conformal bi-layered perovskite/spinel coating on a metallic wire network for solid oxide fuel cells via an electrodeposition-based route, J. Power Sources 348 (2017) 40–47, http://dx.doi.org/10.1016/j.jpowsour.2017.02.080.

[70] M. Kleitz, F. Petitbon, Optimized sofc electrode microstructure, Solid State Ion. 92 (1) (1996) 65–74, http://dx.doi.org/10.1016/S0167-2738(96)00464-X.

[71] M. Kusnezoff, N. Trofimenko, M. Müller, A. Michaelis, Influence of electrode design and contacting layers on performance of electrolyte supported sofc/soec single cells, Materials 9 (11) (2016) http://dx.doi.org/10.3390/ma9110906.